



## Geometric and Causal Structure of Schwarzschild–de Sitter and Kerr–de Sitter Spacetimes

\*<sup>1</sup>Alegbe Taiye Screami, <sup>1</sup>Makama Ezekiel Kaura, <sup>1</sup>Naandoet Bitlin Francis, <sup>1</sup>Algahanuna Abdulhamid Abdullahi, <sup>3</sup>Akerele Domnic Osujeyimi, <sup>2</sup>Percy Karen Awushi, <sup>1</sup>Inuwa Ayuba, <sup>4</sup>Mailafiya Benjamin Yusuf, <sup>1</sup>Maduka Rosemary Chidimma, <sup>1</sup>Tumba Milcah Dabari and <sup>1</sup>Obasiya Danjuma

<sup>1</sup>Department of Physics, Faculty of Natural Sciences, University of Jos, Plateau state, Nigeria.

<sup>2</sup>Department of Accounting, Faculty of Natural Sciences, University of Jos, Plateau State, Nigeria.

<sup>3</sup>Federal College of Fisheries and Marine Technology

<sup>4</sup>Nigerian Building & Road Research Institute, Nigeria.

\*Corresponding Author's Email: [alegbescreami@gmail.com](mailto:alegbescreami@gmail.com) Phone: +2347034431202

### ABSTRACT

We investigate the geometric and causal structure of Schwarzschild-de Sitter and Kerr-de Sitter space times as solutions of Einstein's field equations with a non-zero cosmological constant. Emphasis is placed on the role of the cosmological constant as an active geometric parameter influencing horizon formation, global curvature, and causal accessibility. For the Schwarzschild-de Sitter case, we analyze the existence of multiple horizons and the emergence of a finite static region bounded by the black hole and cosmological horizons, including the Nariai limit as a critical configuration. The Kerr-de Sitter space time is examined to assess the combined effects of rotation and cosmological expansion, highlighting the presence of additional horizons and ergo regions that modify causal structure. Using conformal compactification, Penrose and projection diagrams are constructed to elucidate the global properties of these space times. A particular contribution of this work is the unified comparative treatment of Schwarzschild-de Sitter and Kerr-de Sitter geometries within a common conformal framework, allowing direct comparison of their causal structures and horizon configurations. The results provide a unified geometric framework for understanding  $\Lambda$ -modified black hole space times.

### Keywords:

General Relativity,  
Cosmological Constant,  
Black Hole Space times,  
de Sitter Space,  
Causal Structure.

### INTRODUCTION

The cosmological constant has re-emerged as a central element of modern gravitational physics following observational evidence for the accelerated expansion of the universe (Riess et al., 1998; Perl mutter et al., 1999; Planck Collaboration, 2020). Once introduced by Einstein as a modification of the field equations (Einstein, 1917), the cosmological constant is now understood to encode the large-scale curvature of space time and to play a fundamental role in cosmology (Weinberg, 1989; Carroll, 2001; Bull et al., 2016). In this context, exact solutions of Einstein's field equations with a non-zero cosmological constant provide an essential theoretical laboratory for exploring the interplay between local strong-field gravity and global cosmological effects (Gibbons & Hawking, 1977; Bousso, 2002; Frassino et al., 2023). Among such solutions, black holes embedded in de Sitter backgrounds are of particular interest (Gibbons & Hawking, 1977; Bousso, 2002; Anninos,

2012). Schwarzschild-de Sitter space time represents the simplest model of a non-rotating black hole in an expanding universe (Kottler, 1918; Podolský & Griffiths, 2002), while Kerr-de Sitter space time generalizes this picture to include angular momentum (Carter, 1968; Gibbons et al., 2005). Unlike asymptotically flat black holes, these space times possess multiple horizons, typically including a black hole event horizon and a cosmological horizon, each associated with distinct geometric and causal properties (Gomberoff & Teitelboim, 2003; Urano et al., 2009). The presence of multiple horizons leads to a finite static region and introduces novel features in the global structure of space time that are absent when the cosmological constant vanishes (Bousso, 2002; Akbar & Cai, 2006; Frassino et al., 2023). The causal structure of de Sitter black hole space times is therefore considerably richer than that of their asymptotically flat counterparts (Gibbons & Hawking, 1977; Bousso, 2002; Anninos, 2012). The

existence and relative ordering of horizons depend sensitively on the values of physical parameters such as mass, angular momentum, and the cosmological constant (Podolský & Griffiths, 2002; Stuchlík & Hledík, 1999). In particular, critical configurations such as the Nariai limit, in which the black hole and cosmological horizons coincide, mark transitions in the global geometry and signal important changes in causal accessibility (Nariai, 1950; Bousso & Hawking, 1996; Urano et al., 2009). In rotating space times, additional structures such as ergo regions further modify the causal behavior and influence the motion of observers and fields (Carter, 1968; Gibbons et al., 2005; Grenzebach et al., 2014). Understanding the geometric and causal properties of Schwarzschild-de Sitter and Kerr-de Sitter space times is not only of intrinsic theoretical interest but also provides a foundation for related studies in black hole thermodynamics, quantum field theory in curved space time, and  $\Lambda$ -dominated cosmology (López et al., 2023; Goswami & Narayan, 2024; Armas & Nicosia, 2024). While extensive work has been devoted to the thermodynamic interpretation of de Sitter black holes, particularly in the context of extended phase space and black hole chemistry (Rehan et al., 2024; Hennigar et al., 2025), a clear and comparative treatment of their geometric and causal structure remains valuable, especially in highlighting the role of the cosmological constant as an active geometric parameter rather than a passive background quantity (Frassino et al., 2023; Mann, 2024). In this paper, we present a systematic analysis of the geometric and causal structure of Schwarzschild-de Sitter and Kerr-de Sitter space times. We examine the influence of the cosmological constant on horizon formation, static regions, and global causal properties, employing conformal compactification techniques to construct Penrose and projection diagrams that elucidate the multi-horizon nature of these geometries. By comparing the non-rotating and rotating cases, we clarify the distinct roles played by the cosmological constant and angular momentum in shaping space time structure. The results presented here provide a geometric framework that naturally complements subsequent investigations of horizon thermodynamics and related physical phenomena.

Unlike previous studies that often examine Schwarzschild-de Sitter and Kerr-de Sitter geometries separately, this work develops a unified comparative conformal framework that systematically contrasts their horizon structures, causal accessibility, and global geometric properties.

## MATERIALS AND METHODS

This study adopts a fully theoretical and analytical framework based on Einstein's field equations with a non-zero cosmological constant  $\Lambda$ . Rather than relying on observational or experimental input, the analysis focuses

on exact solutions of the field equations and their geometric and causal properties. In particular, attention is given to spacetimes of cosmological relevance, including de Sitter, anti-de Sitter, Schwarzschild-de Sitter, and Kerr-de Sitter geometries.

The investigation proceeds by examining the structure of maximally symmetric space times and extending this analysis to black hole solutions in the presence of a cosmological constant. The horizon structure is determined by the roots of the metric functions, thereby allowing the identification of black hole and cosmological horizons and the characterization of static regions. The global causal properties of these space times are then analyzed using conformal compactification, which enables the construction of Penrose and projection diagrams that capture the essential features of causal accessibility.

In addition to geometric considerations, selected thermodynamic aspects of space time horizons are incorporated to provide physical context. Quantities such as surface gravity, Hawking temperature, and entropy are evaluated within the standard semi classical framework. At the same time, the cosmological constant is interpreted in the extended phase-space formalism as an effective thermodynamic pressure. These elements are included primarily to support the geometric interpretation of horizon structure rather than to provide a full thermodynamic analysis.

Analytical derivations are supplemented by symbolic computation tools, including Python-based packages such as SymPy, to ensure algebraic consistency and to facilitate the evaluation of curvature quantities and horizon conditions. Overall, the methodology provides a coherent framework for analyzing how the cosmological constant influences both the geometry and causal structure of black hole space times.

## Theoretical Framework

### *The Cosmological Constant in Modern General Relativity*

The cosmological constant ( $\Lambda$ ), originally introduced by Einstein to achieve a static universe, has evolved into a cornerstone of modern cosmology. Once discarded after the discovery of cosmic expansion, the  $\Lambda$  term resurfaced with the observation of the universe's accelerated expansion in the late 1990s. Incorporated into the Einstein field equations as;

$$G_{\mu\nu} + \Lambda g_{\mu\nu} = \frac{8\pi G}{c^4} T_{\mu\nu}, \quad (1)$$

Where:  $G_{\mu\nu}$  is the Einstein tensor, which encapsulates the geometry of spacetime,  $T_{\mu\nu}$  is the energy-momentum tensor, representing the matter and energy content,  $\Lambda g_{\mu\nu}$  represents a uniform energy density permeating space time, interpreted today as dark energy.  $G$  is Newton's gravitational constant, and  $c$  is the speed of light.

Here,  $\Lambda$  acts as a uniform energy density of spacetime, influencing its curvature independently of matter. A positive  $\Lambda$  corresponds to a de Sitter universe, associated with cosmic acceleration, while a negative  $\Lambda$  yields anti-de Sitter spaces, crucial in high-energy theories such as the AdS/CFT correspondence (Witten, 1998). The geometrical effects of  $\Lambda$  are evident in Penrose diagrams, which reveal changes in causal structure, event horizons, and conformal boundaries across different spacetime models.

Beyond its geometric implications,  $\Lambda$  plays a thermodynamic role when interpreted as pressure;

$$P = -\frac{\Lambda}{8\pi G} \tag{2}$$

In the extended phase space of black hole thermodynamics, contributing to phenomena like black hole phase transitions. This reinterpretation has fueled investigations into emergent gravity and the link between space time and entropy (Dolan, 2014; Kubiz̃, 2016). Observationally,  $\Lambda$  is central to the  $\Lambda$ CDM model, supported by data from supernovae, the cosmic microwave background, and large-scale structure surveys. However, deep theoretical challenges remain, particularly the cosmological constant problem, which is why the observed value of  $\Lambda$  is vastly smaller than quantum field theory predicts. As such,  $\Lambda$  continues to bridge general relativity, quantum theory, and cosmology, embodying one of the most profound mysteries in modern physics.

**De Sitter Space-time and Einstein Field Equations**

We consider Einstein’s field equations with a non-zero cosmological constant. We begin with Einstein’s field equations in the presence of a non-zero cosmological constant  $\Lambda$ , given by

$$G_{\mu\nu} + \Lambda g_{\mu\nu} = 8\pi T_{\mu\nu}, \tag{3}$$

Where  $G_{\mu\nu}$  is the Einstein tensor,  $g_{\mu\nu}$  is the spacetime metric, and  $T_{\mu\nu}$  is the energy-momentum tensor (Einstein, 1917; Carroll, 2001). In a vacuum, where  $T_{\mu\nu} = 0$ , the equations reduce to

$$G_{\mu\nu} + \Lambda g_{\mu\nu} = 0. \tag{4}$$

Using the definition of the Einstein tensor,

$$G_{\mu\nu} = R_{\mu\nu} - \frac{1}{2}Rg_{\mu\nu}, \tag{5}$$

The vacuum field equations can be rewritten as

$$R_{\mu\nu} - \frac{1}{2}Rg_{\mu\nu} + \Lambda g_{\mu\nu} = 0 \text{ (Hawking \& Ellis 1973; Wald 1984)}. \tag{6}$$

Taking the trace of this equation by contracting with  $g^{\mu\nu}$ , we obtain

$$R = 4\Lambda, \tag{7}$$

Which, when substituted back, yields

$$R_{\mu\nu} = \Lambda g_{\mu\nu}. \tag{8}$$

This result shows that vacuum solutions with a cosmological constant correspond to space times of constant Ricci curvature. Such space times are maximally

symmetric and are completely characterized by the value of  $\Lambda$  (Weinberg 1972; Carroll 2001).

In vacuum, these equations admit de Sitter space as a maximally symmetric solution, providing the background for black hole generalizations. For a positive cosmological constant  $\Lambda > 0$ , the unique maximally symmetric vacuum solution is de Sitter spacetime, which represents a space time of constant positive curvature and plays a central role in modern cosmology (Gibbons & Hawking, 1977; Spradlin et al., 2001; Anninos, 2012).

In static coordinates, the de Sitter metric can be written as

$$ds^2 = -\left(1 - \frac{\Lambda r^2}{3}\right) dt^2 + \left(1 - \frac{\Lambda r^2}{3}\right)^{-1} dr^2 + r^2 d\Omega^2, \tag{9}$$

$$d\Omega^2 = d\theta^2 + \sin^2 \theta d\phi^2.$$

Where  $d\Omega^2$  is the metric on the unit two-sphere.

The metric function

$$f(r) = 1 - \frac{\Lambda r^2}{3} \tag{10}$$

Vanishes at

$$r_c = \sqrt{\frac{3}{\Lambda}}, \tag{11}$$

Which defines the cosmological horizon (Gibbons & Hawking, 1977; Bousso, 2002). This horizon acts as a causal boundary, beyond which events cannot influence an observer located within the static region.

The curvature structure of de Sitter space time is encoded in the Riemann tensor,

$$R_{\mu\nu\rho\sigma} = \frac{\Lambda}{3}(g_{\mu\rho}g_{\nu\sigma} - g_{\mu\sigma}g_{\nu\rho}), \tag{12}$$

Which confirms that the space time has constant curvature (Wald, 1984; Carroll, 2001). The associated curvature invariants are

$$R = 4\Lambda, \quad R_{\mu\nu}R^{\mu\nu} = 4\Lambda^2, \quad R_{\mu\nu\rho\sigma}R^{\mu\nu\rho\sigma} = \frac{8}{3}\Lambda^2, \tag{13}$$

Demonstrating that de Sitter space time is homogeneous and isotropic.

**Schwarzschild–de Sitter Space-time**

The Schwarzschild-de Sitter solution describes a static, spherically symmetric black hole embedded in a universe with a positive cosmological constant  $\Lambda > 0$ . The metric is given by:

$$ds^2 = -f(r)dt^2 + \frac{dr^2}{f(r)} + r^2 d\Omega^2 \tag{14}$$

Where,

$$f(r) = 1 - \frac{2GM}{r} - \frac{\Lambda r^2}{3}. \tag{15}$$

Here, M represents the mass of the black hole. Unlike the Schwarzschild solution with  $\Lambda = 0$ , the function  $f(r)$  now includes a cosmological term that modifies the gravitational potential at large scales (Ghaffari & Luciano, 2025).

The SdS space time features two distinct horizons: The black hole event horizon, located at the smaller positive root of  $f(r) = 0$  for;

Schwarzschild–de Sitter:

$$1 - \frac{2M}{r} - \frac{\Lambda r^2}{3} = 0.$$

Kerr–de Sitter:

$$\Delta_r = 0 \tag{16}$$

i.e.

$$(r^2 + a^2) \left(1 - \frac{\Lambda r^2}{3}\right) - 2Mr = \Delta_r \tag{17}$$

And the cosmological horizon, found at the larger positive root. Between these horizons lies a static region where observers can exist. The presence of two horizons with different temperatures complicates the thermodynamic analysis and raises questions about the equilibrium states of such systems. The Penrose diagram of SdS reveals a causal structure with multiple regions separated by these horizons, influencing particle trajectories and horizon thermodynamics (Aninos & Harris, 2021).

**Kerr-de Sitter Space-time**

The Kerr-de Sitter (KdS) space time describes a rotating black hole solution of Einstein’s field equations in the presence of a positive cosmological constant  $\Lambda > 0$ . It generalizes the Kerr solution by incorporating cosmological expansion and reduces to the standard Kerr spacetime in the limit  $\Lambda \rightarrow 0$  (Carter 1968; Gibbons et al. 2005; Akcay & Matzner 2011). The inclusion of both angular momentum and a cosmological constant yields a significantly richer geometric and causal structure than the non-rotating Schwarzschild–de Sitter case (Stuchlík & Hledík, 1999; Grenzebach et al., 2014).

In Boyer–Lindquist–type coordinates, the Kerr–de Sitter metric is given by

$$ds^2 = -\frac{\Delta_r}{\rho^2} \left(dt - \frac{a \sin^2 \theta}{\Xi} d\phi\right)^2 + \frac{\rho^2}{\Delta_r} dr^2 + \frac{\rho^2}{\Delta_\theta} d\theta^2 + \frac{\Delta_\theta \sin^2 \theta}{\rho^2} \left(a dt - \frac{r^2 + a^2}{\Xi} d\phi\right)^2, \tag{18}$$

Where the metric functions are defined as;

$$\Delta_r = (r^2 + a^2) \left(1 - \frac{\Lambda r^2}{3}\right) - 2GMr, \tag{19}$$

$$\Delta_\theta = 1 + \frac{\Lambda a^2}{3} \cos^2 \theta, \tag{20}$$

$$\rho^2 = r^2 + a^2 \cos^2 \theta, \tag{21}$$

$$\Xi = 1 + \frac{\Lambda a^2}{3}. \tag{22}$$

(Carter 1968; Gibbons et al. 2005).

Here,  $a$  is the black hole’s spin parameter, related to its angular momentum. The interplay between rotation and  $\Lambda$  introduces a rich causal structure that is significantly modified relative to that of asymptotically flat Kerr black holes (Ladino et al., 2025). Adding angular momentum yields the Kerr-de Sitter solution. Rotation introduces additional structure, including ergo regions and modified horizon behavior, significantly enriching the causal geometry.

**Horizon Structure**

The horizon structure of Kerr-de Sitter space time is determined by the roots of the radial function  $\Delta_r$ .

Horizons are located at the values of  $r$  satisfying

$$\Delta_r = 0.$$

That is,

$$(r^2 + a^2) \left(1 - \frac{\Lambda r^2}{3}\right) - 2Mr = 0. \tag{23}$$

This equation generally admits multiple real roots depending on the values of  $M, a$  and  $\Lambda$ . For physically relevant parameter ranges, the spacetime may contain; an inner (Cauchy) horizon, an outer black hole event horizon  $r_+$ , a cosmological horizon  $r_c$ .

The number and ordering of these horizons depend sensitively on the interplay between rotation and the cosmological constant. As  $\Lambda$  increases, the cosmological horizon moves inward, while increasing rotation modifies the separation and structure of the black hole horizons. In certain limiting cases, horizons may coincide, leading to external configurations analogous to the Nariai limit in the non-rotating case.

**Ergo Regions and Causal Structure**

A distinctive feature of rotating space times is the existence of ergo regions, defined as regions where the time like Killing vector  $\partial_t$  becomes spacelike. In Kerr-de Sitter space time, the boundary of the ergo region (the ergo surface) is determined by the condition.

$$g_{tt} = 0. \tag{24}$$

Within this region, no observer can remain stationary with respect to asymptotic coordinates, and all particles are forced to co-rotate with the black hole due to frame-dragging effects. The presence of a cosmological constant modifies the size and location of the ergo region compared to the asymptotically flat Kerr case.

The coexistence of multiple horizons and ergo regions leads to a highly nontrivial causal structure. In particular, observers are confined to regions bounded by horizons, frame-dragging alters geodesic motion, and causal accessibility is further restricted than in Schwarzschild-de Sitter space time. These features highlight the combined influence of rotation and the cosmological constant in shaping the global geometry of space time.

**Comparison with Schwarzschild–de Sitter**

Compared to the Schwarzschild-de Sitter space time, the Kerr-de Sitter geometry exhibits additional horizons due to rotation, ergo regions absent in the static case, and more complex causal relationships between regions

Thus, while the cosmological constant introduces a cosmological horizon and finite static region in both cases, rotation significantly enriches the space time structure by introducing new geometric and causal features.

### Conformal Structure and Penrose Diagrams

To analyze global causal properties, we employ conformal compactification techniques. Penrose diagrams provide insight into horizon relationships and causal accessibility in both SdS and KdS space times. For Schwarzschild-de Sitter space time, the conformal diagram can be constructed explicitly and reveals the presence of multiple horizons and a finite static region. For Kerr-de Sitter space time, however, the construction of a full global Penrose diagram is significantly more involved due to the absence of spherical symmetry. Accordingly, because of the lack of spherical symmetry, the diagrams presented for Kerr-de Sitter space time should be interpreted as projection diagrams that capture the essential causal features rather than as complete conformal representations.

## RESULTS AND DISCUSSION

### Geometric Modifications of Maximally Symmetric Space Times

We first examine the geometric structure of maximally symmetric space times arising from Einstein's vacuum field equations with a non-zero cosmological constant  $\Lambda$ . For  $\Lambda \neq 0$ , the field equations admit two distinct classes of solutions depending on the sign of  $\Lambda$ .

For  $\Lambda > 0$ , the solution corresponds to de Sitter (dS) spacetime, characterized by constant positive curvature and the presence of a cosmological horizon. The horizon defines a causal boundary beyond which events cannot influence observers within the static region. The exponential expansion associated with de Sitter space time provides a geometric basis for the observed acceleration of the universe.

For  $\Lambda < 0$ , the corresponding solution is anti-de Sitter (AdS) spacetime, which possesses constant negative curvature and a timelike boundary at spatial infinity. Unlike de Sitter space time, AdS does not exhibit a cosmological horizon, but instead has a confining geometry that plays a central role in holographic dualities.

The curvature properties of these space times are encoded in invariant quantities such as the Ricci scalar,  $R = 4\Lambda$ ,

And the Kretschmann scalar, confirming that  $\Lambda$  directly determines the global curvature. These features are illustrated schematically in Fig. 1 through embedding diagrams of de Sitter and anti-de Sitter space times.

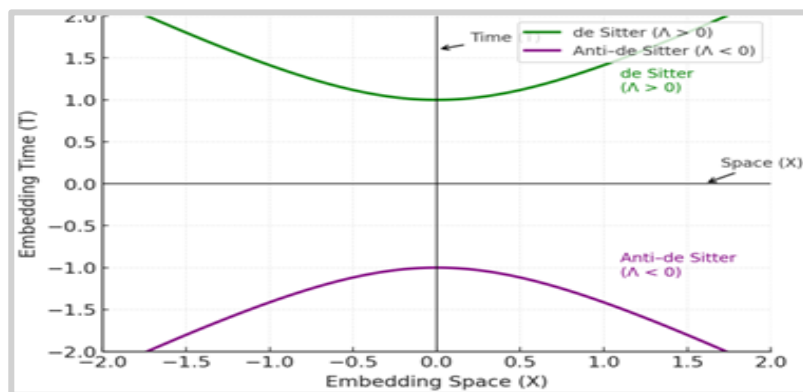


Figure 1: Embedding Diagrams of de Sitter ( $\Lambda > 0$ ) and Anti-de Sitter ( $\Lambda < 0$ ) Spacetimes as Hyperboloids in Higher-Dimensional Minkowski Space

Thus, the findings under this objective demonstrate that  $\Lambda$  is not a passive constant in Einstein's equations but rather an active geometric parameter. Here, a positive  $\Lambda$  yields an expanding universe with horizons, while a negative  $\Lambda$  gives a confining geometry with reflective boundaries.  $\Lambda$  is shown to govern both the symmetry properties and causal boundaries of maximally symmetric space times, bridging classical general relativity with modern ideas in cosmology and holography.

### Horizon Structure and Thermodynamic Quantities of Black Holes

The Schwarzschild-de Sitter space time is characterized by the metric function  $1 - \frac{2M}{r} - \frac{\Lambda r^2}{3} = f(r)$  which provides multiple real roots. The smaller positive root corresponds to the black hole event horizon ( $r_b$ ), while the larger root corresponds to the cosmological horizon ( $r_c$ ). As the cosmological constant increases, the two horizons approach one another until they coincide in the Nariai limit, producing a degenerate configuration. The conformal structure of this space time is illustrated in Fig. 2, which shows the black hole interior, the finite static region, and the cosmological exterior.

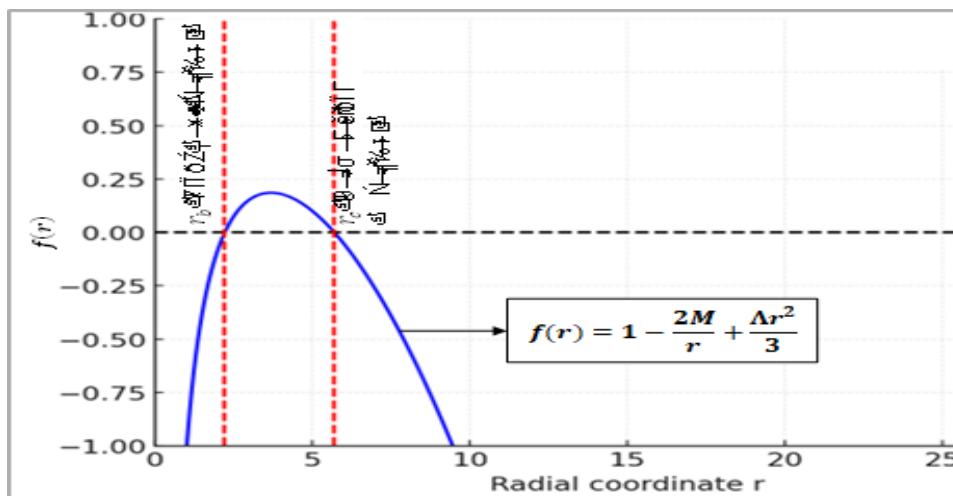


Figure 2: Schwarzschild-de Sitter Horizon Structure Space-time.

**Horizon Structure of Kerr–de Sitter Space-time**

The Kerr–de Sitter (KdS) space time exhibits a more intricate structure due to the presence of angular momentum. The radial horizon structure is determined by the equation

$$\Delta_r = (r^2 + a^2) \left(1 - \frac{\Lambda r^2}{3}\right) - 2Mr = 0.$$

The presence of angular momentum introduces an inner Cauchy horizon, an outer event horizon, and a cosmological horizon, depending on the

parameters  $(M, a, \Lambda)$ . In addition, frame-dragging effects give rise to ergoregions, defined by the condition  $g_{tt} = 0$ , where no static observers can exist. These features underline the richness of Kerr–de Sitter spacetime and its distinct departure from both the pure Kerr and pure de Sitter cases as shown in Figure 3. Additionally, the figure confirmed how both the spin parameter  $a$  and the cosmological constant  $\Lambda$  influence the causal and horizon structures.

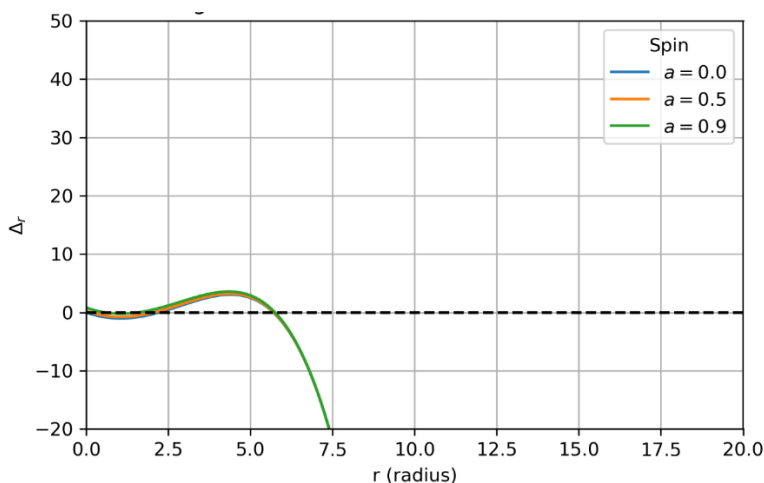


Figure 3: Horizon Structure of Kerr–de Sitter Space-time

The results demonstrate that a positive cosmological constant introduces multiple horizons in both non-rotating and rotating black holes. In the rotating case, additional complexity arises from ergo regions and frame-dragging. These findings indicate that  $\Lambda$  significantly enriches the causal structure of black hole space times.

**Discussion**

The results collectively highlight the influence of the cosmological constant on space time geometry and

horizon structure. In terms of geometry, the cosmological constant was shown to act as a fundamental switch. A positive  $\Lambda$  generates the exponentially expanding de Sitter space time, which is central to both early-universe inflation and present-day cosmic acceleration. Conversely, a negative  $\Lambda$  produces anti-de Sitter space time, which is of immense theoretical interest due to its time-like boundary and role in the AdS/CFT. The result agrees with the findings of Maldacena (1998) and Witten (1998). Generally, these results confirm that  $\Lambda$

determines whether the universe evolves as an expanding, horizon-limited system or as a confining, holographic ally dual system.

The horizon analysis reinforced this dual role. Schwarzschild-de Sitter black holes exhibit two distinct horizons, whose causal boundaries shape the static patch available to observers. The Nariai limit illustrates a critical configuration that has been widely studied in semi-classical gravity. The addition of rotation in Kerr-de Sitter black holes further enriched the horizon dynamics, producing ergo regions and highlighting the interplay between mass, angular momentum, and the cosmological constant. These results are consistent with previous studies (Gibbons & Hawking, 1977; Anninos & Harris, 2021; Ladino et al., 2025) but extend them by emphasizing the thermodynamic implications of multiple horizons.

The results demonstrate that the cosmological constant acts as an active geometric parameter, fundamentally altering space time structure. Rotation further modifies causal features, highlighting differences between SdS and KdS geometries.

## CONCLUSION

This study presents a comparative geometric and causal analysis of Schwarzschild-de Sitter and Kerr-de Sitter space times within Einstein's field equations with a non-zero cosmological constant. The results show that the cosmological constant acts as an active geometric parameter governing horizon formation, causal accessibility, and global space time curvature. For Schwarzschild-de Sitter space time, the analysis reveals distinct black hole and cosmological horizons, separated by a finite static region, with the Nariai limit marking a critical configuration in which the horizons merge. For Kerr-de Sitter space time, angular momentum introduces additional causal features, including ergo regions, frame dragging, and more complex horizon structures. The conformal and projection diagrams constructed in this work provide a unified visualization of these causal properties. Overall, the findings highlight the combined influence of cosmological expansion and rotation on space time geometry and establish a foundation for future studies of horizon thermodynamics, quantum field effects, and black hole phase behavior in  $\Lambda$ -dominated space times.

## REFERENCES

Akçay, S., & Matzner, R. A. (2011). The Kerr-de Sitter universe. *Classical and Quantum Gravity*, 28(8), 085012. <https://doi.org/10.1088/0264-9381/28/8/085012>

Anninos, D. (2012). De Sitter musings. *International Journal of Modern Physics A*, 27(12), 1230013. <https://doi.org/10.1142/S0217751X1230013X>

Bousso, R. (2002). Adventures in de Sitter space. arXiv preprint arXiv:hep-th/0205177. Available at: <https://arxiv.org/abs/hep-th/0205177>

Bull, P., et al. (2016). Beyond  $\Lambda$ CDM: Problems, solutions, and the road ahead. *Physics of the Dark Universe*, 12, 56–99. <https://doi.org/10.1016/j.dark.2016.02.001>

Carroll, S. M. (2001). The cosmological constant. *Living Reviews in Relativity*, 4(1), 1. <https://doi.org/10.12942/lrr-2001-1>

Carter, B. (1968). Global structure of the Kerr family of gravitational fields. *Physical Review*, 174(5), 1559–1571. <https://doi.org/10.1103/PhysRev.174.1559>

Dolan, B. P. (2014). The cosmological constant and black hole thermodynamics. *Classical and Quantum Gravity*, 31(3), 035022. <https://doi.org/10.1088/0264-9381/31/3/035022>

Einstein, A. (1917). Kosmologische Betrachtungen zur allgemeinen Relativitätstheorie. *Sitzungsberichte der Königlich Preußischen Akademie der Wissenschaften*, 142–152.

Frassino, A. M., Pedraza, J. F., Svesko, A., & Visser, M. R. (2023). Higher-dimensional origin of extended black hole thermodynamics. *Physical Review Letters*, 130(16), 161501. <https://doi.org/10.1103/PhysRevLett.130.161501>

Gibbons, G. W., & Hawking, S. W. (1977). Cosmological event horizons, thermodynamics, and particle creation. *Physical Review D*, 15(10), 2738–2751. <https://doi.org/10.1103/PhysRevD.15.2738>

Gomberoff, A., & Teitelboim, C. (2003). de Sitter black holes with either of the two horizons as a boundary. *Physical Review D*, 67(10), 104024. <https://doi.org/10.1103/PhysRevD.67.104024>

Grenzebach, A., Perlick, V., & Lämmerzahl, C. (2014). Photon regions and shadows of Kerr–Newman–NUT black holes. *Physical Review D*, 89(12), 124004. <https://doi.org/10.1103/PhysRevD.89.124004>

Hawking, S. W., & Ellis, G. F. R. (1973). *The large scale structure of space-time*. Cambridge University Press. <https://doi.org/10.1017/CBO9780511524646>

Kottler, F. (1918). Über die physikalischen Grundlagen der Einsteinschen Gravitationstheorie. *Annalen der Physik*, 361(14), 401–462. <https://doi.org/10.1002/andp.19183611402>

Kubizňák, D., & Mann, R. B. (2012). P–V criticality of charged AdS black holes. *Journal of High Energy Physics*, 2012(7), 033. [https://doi.org/10.1007/JHEP07\(2012\)033](https://doi.org/10.1007/JHEP07(2012)033)

Nariai, H. (1950). On a new cosmological solution of Einstein's field equations. *Science Reports of the Tohoku University, Series I*, 34, 160–167. <https://cir.nii.ac.jp/crid/1571417125948039040>

Planck Collaboration. (2020). Planck 2018 results. VI. Cosmological parameters. *Astronomy & Astrophysics*, 641, A6. <https://doi.org/10.1051/0004-6361/201833910>

Podolský, J., & Griffiths, J. B. (2002). Accelerating Kerr–Newman black holes in (anti-)de Sitter spacetime. *Physical Review D*, 63(2), 024006. <https://doi.org/10.1103/PhysRevD.63.024006>

Rehan, M., Khan, S., & Abbas, G. (2024). Thermodynamic behavior of de Sitter black holes in extended phase space. *Scientific Reports*, 14, 62645. <https://doi.org/10.1038/s41598-024-62645-4>

Stuchlík, Z., & Hledík, S. (1999). Some properties of Schwarzschild–de Sitter and Schwarzschild–anti–de Sitter spacetimes. *Physical Review D*, 60(4), 044006. <https://doi.org/10.1103/PhysRevD.60.044006>

Urano, M., Tomimatsu, A., & Saida, H. (2009). Mechanical first law of black hole spacetimes with cosmological constant. *Classical and Quantum Gravity*, 26(10), 105010. <https://doi.org/10.1088/0264-9381/26/10/105010>

Weinberg, S. (1972). *Gravitation and cosmology: Principles and applications of the general theory of relativity*. Wiley. Weinberg, S. (1972). Available at: <https://www.worldcat.org/search?q=Weinberg+Gravitati+on+and+Cosmology+1972>

Weinberg, S. (1989). The cosmological constant problem. *Reviews of Modern Physics*, 61(1), 1–23. <https://doi.org/10.1103/RevModPhys.61.1>

Witten, E. (1998). Anti-de Sitter space and holography. *Advances in Theoretical and Mathematical Physics*, 2(2), 253–291. <https://arxiv.org/pdf/hep-th/9802150>